Journal of Cell Science 109, 2031-2040 (1996)
Printed in Great Britain © The Company of Biologists Limited 1996
JCS7096

Actin filament bundles are required for microtubule reorientation during growth cone turning to avoid an inhibitory guidance cue

Jean F. Challacombe*, Diane M. Snow and Paul C. Letourneau

The University of Minnesota, Department of Cell Biology and Neuroanatomy, 321 Church St SE, 4-135 Jackson Hall, Minneapolis, MN 55455, USA

*Author for correspondence (e-mail: jchalla@lenti.med.umn.edu)

SUMMARY

The extracellular matrix through which growth cones navigate contains molecules, such as chondroitin sulfate proteoglycan, that can inhibit growth cone advance and induce branching and turning. Growth cone turning is accompanied by rearrangement of the cytoskeleton. To identify changes in the organization of actin filaments and microtubules that occur as growth cones turn, we used time-lapse phase contrast videomicroscopy to observe embryonic chick dorsal root ganglion neuronal growth cones at a substratum border between fibronectin and chondroitin sulfate proteoglycan, in the presence and absence of cytochalasin B. Growth cones were fixed and immunocytochemically labeled to identify actin filaments and dynamic and stable microtubules.

Our results suggest that microtubules are rearranged within growth cones to accomplish turning to avoid chondroitin sulfate proteoglycan. Compared to growth cones migrating on fibronectin, turning growth cones were more narrow, and they contained dynamic microtubules that were closer to the leading edge and were more bundled. Cytochalasin B-treated growth cones sidestepped laterally along the border instead of turning, and in sidestepping growth cones, microtubules were not bundled and aligned. We conclude that actin filament bundles are required for microtubule reorientation and growth cone turning to avoid chondroitin sulfate proteoglycan.

Key words: Actin filament, Microtubule, Chondroitin sulfate proteoglycan, Growth cone, Turning

INTRODUCTION

Neuronal growth cones navigate by responding to complex molecular signals, including both positive and negative guidance cues that are secreted (Kennedy and Tessier-Lavigne, 1995; Lumsden, 1992; O'Leary et al., 1991), expressed on cell surfaces (Goodman et al., 1992; Letourneau, 1992; Letourneau and Shattuck, 1989), and/or are components of the extracellular matrix (ECM) (Letourneau et al., 1994; Reichardt and Tomaselli, 1991; Sanes, 1989). Chondroitin sulfate proteoglycans (CSPGs) are transiently expressed in regions that exclude axons, both during development of the nervous system and following nervous system injury (Brittis et al., 1992; McKeon et al., 1991; Oakley and Tosney, 1991; Pindzola et al., 1993; Snow et al., 1990, 1991). CSPGs also inhibit growth cone advance from several neuronal types in vitro (Meiners et al., 1995; Snow et al., 1990, 1991; Snow and Letourneau, 1992). When growth cones contact substratum-bound CSPG, the resulting behaviors are branching and turning. These behaviors depend on the organization and dynamics of the major cytoskeletal components of growth cones, actin filaments (AFs) and microtubules (MTs).

Growth cones can be divided into two distinct regions. The peripheral, or P-domain, consists of a thin region from which the motile and sensory lamellipodia and filopodia emerge. AFs are organized into bundles in filopodia, or into networks that extend throughout lamellipodia (Letourneau and Ressler, 1983; Lewis and Bridgman, 1992). The central, or C-domain adjoins the neurite, and contains the advancing MTs and membranous organelles (Bridgman, 1992). MTs extend into the P-domain, where they overlap with AF bundles at the bases of filopodia (Gordon-Weeks, 1991; Letourneau and Ressler, 1983), suggesting a relationship between AFs and MT organization in growth cones. Whether AFs promote or inhibit the selective advance of MTs into the P-domain is currently unresolved, but several recent studies indicate that AF bundles regulate MT advance (Lin and Forscher, 1993; O'Connor and Bentley, 1993; Smith, 1994). Current hypotheses suggest that cell adhesion molecules of the ECM couple to AFs through 'clutch' protein complexes (Lin et al., 1994; Mitchison and Kirschner, 1988), that, when disengaged, allow AFs to be transported rearward, or when engaged by adhesive contacts, allow interactions with myosin molecules to produce tension that locally promotes MT and growth cone advance.

Growth cone turning is an important behavior, responsible for changing the direction of neurite elongation in several in vivo situations (Oakley and Tosney, 1991; Sabry et al., 1991; Sretavan and Reichardt, 1993). A key event in growth cone turning may be the local realignment and advance of MTs (Lin et al., 1994; Mitchison and Kirschner, 1988; Sabry et al., 1991; Tanaka and Sabry, 1995), to establish the dominant side of a turning growth cone. When a growth cone contacts a positive

guidance cue, filopodia become stabilized in the direction of neurite elongation, and MTs are locally reoriented and advance toward the contact site (Bentley and O'Connor, 1994; Lin and Forscher, 1993; O'Connor and Bentley, 1993; Sabry et al., 1991). In a similar manner, AFs and MTs of growth cones may interact to accomplish turning away from a negative cue, such as substratum-bound CSPG.

The goals of the present study were: (1) to analyze changes in the organization of AFs and MTs in turning growth cones; and (2) to use cytochalasin B (CB) to determine the role of AFs in MT reorganization and growth cone turning. Results show that: (1) growth cone turning is accompanied by changes in MT bundling and alignment; (2) CB-treated growth cones are deficient in AFs and sidestep laterally along fibronectin (FN)/CSPG borders in an abnormal avoidance response; and (3) MTs are not reorganized in CB-treated growth cones. These results suggest that AFs play an important role in MT reorientation and growth cone turning to avoid substratum-bound CSPG. Part of this work has been presented in abstract form (Challacombe et al., 1995).

MATERIALS AND METHODS

Preparation of substrata

Heat-treated glass coverslips (24 mm × 30 mm) were mounted over 22 mm holes drilled into the bottom of 50 mm × 9 mm tissue culture dishes (Falcon Labware, Oxnard, CA) using aquarium sealant (Perfecto Manufacturing, Noblesville, IN). Coverslips were UV sterilized for 30 minutes, coated with 0.1 mg/ml poly-L-lysine for 1 hour at 40°C, rinsed, and coated with nitrocellulose as described previously (Lagenaur and Lemmon, 1987; Snow et al., 1990). Cellulose filter paper strips (Whatman No. 1) were soaked in a solution of chick limb bud CSPG (a generous gift from Drs A. I. Caplan and D. A. Carrino: Carrino and Caplan, 1985) containing 20% RITC, transferred to nitrocellulose-coated dishes (Snow et al., 1990), overlaid with 40-50 μg/ml human plasma FN (in PBS, pH 7.1; gift from Dr J. McCarthy, University of Minnesota), and incubated for 3-4 hours at room temperature or overnight at 4°C. Dishes were subsequently blocked with 5 mg/ml bovine serum albumin in PBS for 1 hour.

Tissue culture

Dorsal root ganglia (DRG) were dissected from embryonic day 9-11 white Leghorn chicken embryos, and cut into pieces to make explants. Explants were suspended in supplemented serum-free Hepes-buffered F14 medium (Letourneau et al., 1990). Dishes containing 20-25 explants were incubated at 40°C in a humidified air chamber for 16 to 48 hours.

Videomicroscopy

Following incubation, a culture dish was placed on the stage of an inverted microscope (Diaphot, Nikon Inc., Garden City, NY), under an air curtain incubator (ASI 400, Carl Zeiss, Thornwood, NY) at 40°C. Growth cones were viewed by phase contrast optics while rhodamine-labeled CSPG stripes were located under epi-illumination. Time-lapse phase contrast images were acquired with a Newvicon video camera (Dage-MTI, Michigan City, IN), enhanced using Image 1 software (Universal Imaging, West Chester, PA), and recorded with an optical disc recorder (Panasonic TQ-2026F or TQ-3038F, Panasonic Industrial Corp., Secaucus, NJ).

Images of a microscope field containing several growth cones approaching a CSPG stripe were recorded once per minute until the growth cones were 100 μm from the CSPG border. Then CB (Sigma, St Louis), dissolved in dimethyl sulfoxide (DMSO), was added to the culture medium, at concentrations of DMSO that did not exceed 3 μl/ml. The same volume of DMSO alone was added to control cultures.

Fixation and immunocytochemistry

To preserve MT integrity, cultures were fixed and extracted simultaneously for 10 minutes with PHEM buffer (Letourneau and Ressler, 1983; Schliwa and van Blerkom, 1981) containing 0.2% glutaraldehyde and 0.1% Triton X-100, followed by one 15 minute treatment with 1 mg/ml sodium borohydride in Ca^{2+}-Mg^{2+}-free PBS (CMF-PBS), and incubation for 15 minutes in soaking solution (CMF-PBS containing 5 mg/ml bovine serum albumin and 1 mg/ml sodium azide). MTs were labeled with rat monoclonal antibody YL 1/2 directed against tyrosinated α-tubulin (Kilmartin et al., 1982; Sera-Labs) and rabbit polyclonal antibody against detyrosinated α-tubulin (a generous gift from Drs J. C. Bulinski and G. G. Gundersen (Gundersen et al., 1984)), used at 1:25 and 1:400 dilutions, respectively. Actin filaments were labeled with rhodamine-conjugated phalloidin (Molecular Probes, Eugene, OR). Primary antibodies and phalloidin were diluted into soaking solution, and applied for 45 minutes. Dishes were rinsed with CMF-PBS to remove unbound antibodies, then soaked for 15 minutes in soaking solution supplemented with 0.5% nonfat dry milk. Fluorescein- and CY5-conjugated secondary antibodies (Jackson ImmunoResearch Laboratories, West Grove, PA), at 1:400 dilutions, were applied simultaneously for 45 minutes. Dishes were rinsed, soaked and coverslipped in a solution containing polyvinyl alcohol and glycerol.

Confocal microscopy

Immunofluorescence images were acquired with a Bio-Rad MRC 1000 confocal laser scanning microscope (Bio-Rad Microscience, Cambridge, MA), equipped with an Optiphot-2 microscope, Planapochromatic ×60/1.4 NA objective (Nikon, Inc.), and krypton-Argon laser (Brelje et al., 1993). To ensure that double and triple labeled images were in the greatest possible register, green, red and/or far red fluorescence images were acquired with the same dichroic mirror. Digital images were reproduced using Adobe Photoshop 3.0.

Quantitation of MT organization in growth cones

To quantitatively examine the organization of MTs in untreated and CB-treated growth cones, images of tyrosinated and detyrosinated α-tubulin MT labeling were merged with images of phalloidin staining to view the positioning of dynamic and stable MTs within the growth cone relative to the leading edge and filopodia. Several growth cone parameters were measured using the Bio-Rad MRC 600 confocal microscope operating software (version 1.22). For each condition, measurement data were pooled, and differences were assessed by the Mann-Whitney test (Mosteller and Rourke, 1973).

To measure growth cone symmetry, a line was drawn that bisected the neurite axis, beginning 20-30 μm proximal to the growth cone and projecting distally through the growth cone. The linear distances from the left and right lateral edges of the leading margin to the bisecting line were measured, and a ratio of the two distances was calculated. Ratio values close to 1 indicated symmetry.

RESULTS

Immunocytochemical analysis of the distribution of AFs and MTs in turning growth cones

To identify the cytoskeletal changes that occur as growth cones turn, we examined the distributions of AFs and MTs in growth cones: (1) migrating on homogeneous FN; (2) approaching stripes of substratum-bound CSPG; (3) interacting with the FN/CSPG border; (4) turning; and (5) migrating along the

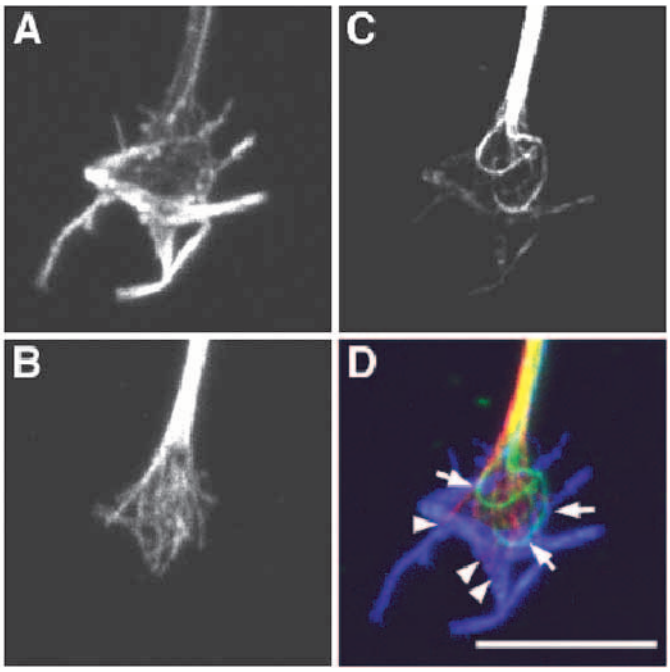

Fig. 1. Triple immunofluorescence of AFs and MTs in a chick DRG growth cone migrating on FN. Confocal images of (A) rhodamine phalloidin-labeled AFs, (B) tyrosinated α-tubulin (dynamic MTs), and (C) detyrosinated α-tubulin (stable MTs) were merged, in three colors (D), to show labeling of stable MTs (green) and dynamic MTs (red) relative to AFs (blue). Based on their size and appearance, the MTs in these images are most likely single or in small bundles. Stable MTs are confined to the central region, where they form loops (D, arrows), while dynamic MTs overlap with AFs at the bases of filopodia (D, arrowheads). Bar, 10 μm.

CSPG border on FN. In several experiments, live growth cones were recorded, then fixed and immunofluorescently stained to label AFs and dynamic and stable MTs.

As stable MT polymers persist in cells, they stain more strongly with antibodies against detyrosinated α-tubulin, and become less reactive with antibodies against tyrosinated α-tubulin (Arregui et al., 1991; Baas and Black, 1990; Brown et al., 1993; Gundersen et al., 1984; Webster et al., 1987). Many neurite MTs are composed of a stable proximal portion and a dynamic distal tip. Newly stabilized MT polymers in axons still contain relatively high levels of tyrosinated α-tubulin (Baas et al., 1993), as demonstrated by local differences in labeling with antibodies against tyrosinated and detyrosinated α-tubulin. Because of the tight bundling and variable lengths of neuritic MTs, we could not resolve antibody labeling of individual MTs in neurites. However, in growth cones migrating on homogeneous FN, there were distinct differences in the labeling of some individual MTs with anti-tyrosinated and anti-detyrosinated α-tubulin antibodies. Dynamic MTs, labeled by anti-tyrosinated α-tubulin antibodies (Fig. 1B), projected from the C-domain into the P-domain, where their distal ends overlapped with AF-rich regions at the bases of filopodia that were intensely stained by phalloidin (Fig. 1D, arrowheads). Stable MTs, labeled by anti-detyrosinated but not by anti-tyrosinated α-tubulin antibodies, were confined to the central region and often displayed a looped configuration (Fig. 1C and D, arrows). AFs were present in the P-domain at the leading edge, and extended as bundles within filopodia (Fig. 1A). Regional differences in the distributions of these cytoskeletal components are more clearly seen in Fig. 1D, where AFs are shown in blue, dynamic MTs in red and stable MTs in green.

As shown in previous studies, when DRG growth cones contacted CSPG, they interacted with it by continuous filopodial sampling, bending, moving laterally through the liquid medium, and retracting, whereby growth cone filopodia repeatedly touched and pulled away from CSPG (Snow et al., 1991, 1994). Importantly, although CSPG inhibited growth cone advance, growth cones rarely collapsed. Rather, the filopodial behaviors that occurred during growth cone interactions with CSPG were confined to individual filopodia, resembling the normal sampling behavior of growth cones that were migrating on homogeneous FN. Confocal images of a recorded growth cone (Fig. 2) show that many filopodia containing AF bundles extended onto the CSPG substratum (Fig. 2A, arrows in Fig. 2C), while in all of the growth cones examined (n>100) dynamic MTs never crossed a border (Fig. 2B, arrowheads).

The turning growth cone in Fig. 3 was not recorded, but is a representative example of cytoskeletal organization, where tightly bundled MTs were aligned along the border in the direction of the turn, and AFs were concentrated at the distal tip (Fig. 3A). In certain regions of turning growth cones, the labeling of dynamic MTs (Fig. 3B) overlapped with labeling of stable MTs (Fig. 3C), indicated by the yellow areas in Fig. 3D. The detyrosinated α-tubulin staining includes some dim nonspecific fluorescence in the distal region of the growth cone that is due to the secondary antibody. However, the specific labeling of stable MTs did not extend as far forward as that of dynamic MTs (arrow in Fig. 3D). Fig. 3 illustrates two important characteristics of turning growth cones: the tight bundling of dynamic MTs (red), and their extension into actin dense regions (blue) at the growth cone tip (arrowhead in Fig. 3D).

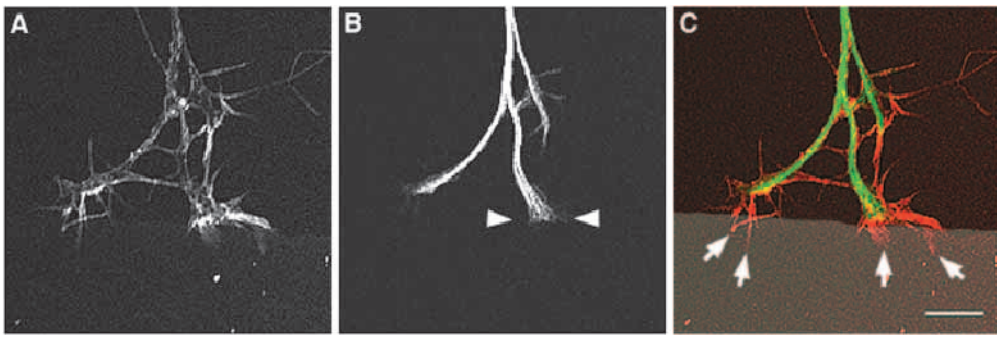

Fig. 2. Distribution of AFs and dynamic MTs in a growth cone at a FN/CSPG border. (A) phalloidin-labeled AFs; (B) anti-tyrosinated α-tubulin. A merged image of the two labels (C) shows that AF bundles of filopodia (red) reach across the border onto CSPG (C, arrows), while dynamic MTs (green) stop at the border (B, arrowheads). Bar, 10 μm.

Fig. 4 shows a non-recorded growth cone that turned and appeared to be migrating on FN along the FN/CSPG border. The arrangement of AFs (Fig. 4A) and dynamic (Fig. 4B) and stable MTs (Fig. 4C) was similar to growth cones migrating on homogeneous FN. This suggests that, once growth cones have turned, the cytoskeleton returns to an organization that is associated with migration on homogeneous FN.

Quantitative analysis of the distribution of AFs and MTs in turning growth cones

In order to better examine changes in MT organization during turning, we quantitatively analyzed the relationship between dynamic and stable MTs and growth cone morphology. Several parameters were measured and compared: (1) distance from leading edge excluding filopodia to distal ends of dynamic MTs; (2) distance from leading edge to distal loops of stable MTs; (3) distance between the distal extents of dynamic and stable MTs; (4) width of dynamic MT staining at the widest point; (5) width of stable MT staining at the widest point; and (6) width of the growth cone at the widest point. The distance from the leading edge to the distal ends of dynamic MTs indicates the portion of the P-domain that has no MTs, the distance from the leading edge to the distal loops of stable MTs is an estimate of the size of the P-domain (which does not contain stable MTs), and the distance between the distal extents of dynamic and stable MTs is an estimate of the portion of MTs that are dynamic.

Results of this analysis (Table 1) showed that, compared to growth cones migrating on homogeneous FN, the dynamic MTs in turning growth cones were closer to the leading edge ($P<0.001$). This suggests that dynamic MTs occupy more of the P-domain and are available to interact more with AFs. Stable MTs also appeared to be closer to the leading edge, but the difference was not statistically significant ($P>0.1$). The dynamic portion of MTs was similar in growth cones that were migrating on homogeneous FN and those that were turning. Also shown in Table 1, the mean width of growth cones decreased ($P<0.001$) during turning. In similar fashion, the mean width of dynamic MT staining decreased ($0.1>P>0.05$). Because the growth cone width also decreased, the degree of MT divergence or splaying did not change appreciably (Fig. 5). Taken together, these results indicate that turning growth cones contain dynamic MTs that are more bundled and are closer to the leading edge, where their organization may be influenced by AFs.

Cytochalasin B alters the behavior of growth cones at FN/CSPG borders

To characterize normal growth cone turning behavior, we reviewed the videorecords of control growth cones from the time that they first contacted CSPG until they turned. Behaviors were grouped as follows: (1) stopping at the border for at least 3 minutes; (2) sidestepping, where the growth cone moves laterally along the border; (3) turning, where the growth cone reorients at the border and begins to migrate along it; (4) sidestepping then turning; (5) turning then sidestepping; (6) complex behaviors, consisting of intermittent episodes of sidestepping, stopping and/or turning.

The results of this analysis (Table 2) show that a majority of the control growth cones observed (57%) exhibited two simple behaviors: (1) turning, or (2) sidestepping, followed by turning. Growth cones spent a variable amount of time at the border (from 4 minutes to 6.4 hours) prior to turning. All of the growth cones that displayed complex behaviors were followed for 7.5-16.6 hours, and it is possible that growth cones exhibited such behaviors for longer periods. However, observations of explant cultures for up to 48 hours after plating consistently revealed that over 80% of control growth cones avoided CSPG by turning (Snow et al., 1990, 1991, and current study).

We examined the role of AFs in growth cone turning by using the drug cytochalasin B (CB), which inhibits addition of actin monomer to filaments (Cooper, 1987; MacLean-Fletcher and Pollard, 1980). CB treatment reduces growth cone filopodial extension in a dose-dependent fashion (Chien et al., 1993; Letourneau et al., 1987; Marsh and Letourneau, 1984), and impairs in vivo growth cone navigation in *Xenopus* (Chien et al., 1993) and grasshopper (Bentley and Toroian-Raymond, 1986) embryos.

As previously found (Letourneau et al., 1987), growth cones

Table 1. Quantitation of MT organization in growth cones migrating on FN and interacting with a CSPG border in the presence and absence of 0.1 μg/ml CB

Treatment	Leading edge to dynamic	Leading edge to stable	Width dynamic	Width stable	Width growth cone
Migrating on FN	7.53±0.39 (117)	10.19±0.44 (115)	7.99±1.28 (23)	3.99±0.80 (23)	22.84±1.99 (21)
Turning	5.86±0.43 (77)	8.99±0.56 (70)	4.67±0.68 (23)	2.09±0.27 (23)	11.46±1.47 (23)
CB (0.1 μg/ml)	1.62±0.14 (214)	5.95±0.28 (146)	22.56±3.0 (24)	14.21±2.57 (22)	26.12±3.46 (24)
Migrating on FN	0.92±0.11 (115)	3.77±0.28 (57)	11.0±1.78 (18)	7.46±1.60 (15)	13.96±1.78 (18)
CB (0.1 μg/ml) At CSPG border					

Distances were measured on merged images of growth cones that were triple labeled for AFs, stable and dynamic MTs. The position of the leading edge and filopodia were ascertained from phalloidin-labeled AFs. The measurement categories represent mean ± s.e.m distances in μm: (1) from the leading edge to the front of dynamic MT labeling; (2) from the leading edge to the front of stable MT labeling; (3) the width of dynamic MT labeling at the widest point; (4) the width of stable MT labeling at the widest point; and (5) the growth cone width at the widest point. Because CB-treated growth cones did not have filopodia, measurements from the leading edge of control growth cones did not include filopodia. To accurately define the distal edges of dynamic and stable MTs, individual images were enhanced prior to merging so that the specific staining of MTs was clearly separable from background staining. For each category, the number of measurements is given in parentheses. The Mann-Whitney test was used to assess the significance of differences between the distributions of measurements in each category.

Table 2. Effect of cytochalasin B on growth cone behavior at FN/CSPG borders

Treatment	Stopped	Sidestepped	Turned	Sidestepped then turned	Turned then sidestepped	Complex
DMSO only	0%	17% (4)	13% (3)	44% (10)	4% (1)	22% (5)*
Cytochalasin B (0.1 μg/ml)	0%	40% (10)	0%	0%	0%	60% (15)†

*Complex behaviors of control growth cones included stopping, sidestepping and turning.
†For cytochalasin B-treated growth cones, complex behaviors consisted of stopping and sidestepping.

exposed to 0.1 μg/ml CB exhibited diminished protrusive activity with a notable absence of filopodia, and migrated on FN at about one-third the normal rate. Importantly, CB-treated growth cones did not turn to avoid CSPG, but moved laterally or 'sidestepped' along the border (Table 2). Fig. 6 illustrates this sidestepping behavior. A fascicle containing three growth cones migrating on FN (Fig. 6A) contacted a CSPG border (Fig. 6B), split into individual growth cones (Fig. 6C); two of the growth cones subsequently sidestepped 38 μm (top growth cone) and 17.6 μm (bottom growth cone), while the third (middle growth cone) stalled at the border. The behaviors of CB-treated growth cones consisted of stopping and sidestepping, or periods of both behaviors (Table 2). Individual CB-treated growth cones were observed for up to 28 hours; however, they never turned.

Effects of CB on the distribution of actin and MTs in growth cones migrating on FN

Following phase contrast videomicroscopy, where possible, recorded growth cones were relocated, and immunofluorescence images acquired. For example Fig. 6D shows the organization of dynamic MTs in a sidestepping growth cone that was recorded prior to fixation. These MTs are splayed with some ends facing the direction of lateral movement.

Confocal images show that phalloidin fluorescence was concentrated in several areas at the leading edge of CB-treated growth cones, but was not organized into the linear staining that is characteristic of the well-organized AF bundles of normal filopodia (Fig. 7A,E,I). Reduction of the AF network is associated with MT extension to the leading margin of the growth cone (Forscher and Smith, 1988; Letourneau et al., 1987). Our confocal images show that these distally projecting MTs are dynamic (Fig. 7D,H,L arrows), and that stable MTs (Fig. 7C,G,K) are generally excluded from the actin-dense regions (compare green/yellow areas to blue areas in Fig. 7D,H,L).

Table 1 shows comparisons of MT organization in untreated and CB-treated growth cones, obtained by measuring the distance from the leading edge to the distal extents of (1) dynamic, and (2) stable MTs, (3) the distance between dynamic and stable MTs, (4) the width of dynamic MT staining, (5) the width of stable MT staining, and (6) the width of the growth cone at the widest point. The quantitative data presented in Table 1 show that for growth cones migrating on homogeneous FN, the mean distance from the leading edge to the distal extents of both dynamic and stable MTs was substantially decreased by CB treatment ($P<0.001$). There was a small, yet significant ($0.05>P>0.02$), increase in the distance between the distal ends of dynamic and stable MTs, suggesting that the proportion of growth cone MTs that were dynamic was increased in the presence of CB. While the maximum width of the growth cone was not significantly changed in the presence of CB ($P>0.2$), the width of both dynamic and stable MT staining increased substantially ($P<0.001$). Thus, the degree of both dynamic and stable MT splaying was increased in CB-treated growth cones (Fig. 5). These data indicate that the dynamic and stable MTs in CB-treated growth cones were closer to the leading edge, and were more splayed.

Effects of CB on the distribution of MTs in growth cones at CSPG borders

When compared to control growth cones that were turning, CB-treated growth cones at a CSPG border showed two major differences in MT distribution (Table 1). Dynamic and stable MTs were closer to the leading edge ($P<0.001$), and the degree of MT splaying was increased (Fig. 5). To illustrate these findings, Fig. 7L shows a growth cone that was not recorded prior to fixation, but has a morphology representative of sidestepping growth cones. By comparing recorded growth cones, we determined that CB-treated growth cones at CSPG borders for prolonged periods of time had an identical morphology and cytoskeletal arrangement, whether they were stopped or sidestepping. In these growth cones, many dynamic MTs were right at the leading edge (Fig. 7L, arrows). In addition, dynamic MTs were not tightly bundled, but were splayed across the width of the growth cone.

Compared to CB-treated growth cones on homogeneous FN, dynamic and stable MTs in CB-treated growth cones at a CSPG border were significantly closer to the leading edge (Table 1; $P<0.001$). Interestingly, the distance between dynamic and stable MTs was smaller in growth cones at the CSPG border compared to those migrating on homogeneous FN ($P<0.001$), suggesting that the region occupied only by dynamic MTs was reduced in CB-treated growth cones following contact with CSPG. Compared to CB-treated growth cones on homogeneous FN, CB-treated growth cones interacting with CSPG were more narrow ($P<0.02$), and contained dynamic MTs that were slightly less splayed (Fig. 5). However, when compared to untreated growth cones, the MTs in CB-treated growth cones were always more splayed, and MTs, especially the dynamic MTs, were closer to the front margin.

Measurements of growth cone symmetry (not shown) revealed that CB-treated growth cones at a border were as symmetric as those migrating on homogeneous FN (compare Fig. 7D,L). This is in contrast to the obvious asymmetry that arises in control growth cones when they begin to turn (Fig. 3). These results show that, in addition to being more splayed, the MTs in CB-treated growth cones were not aligned to one side of the growth cone, as they were in turning growth cones.

Latrunculin B inhibits AF polymerization by a different mechanism from the cytochalasins (Spector et al., 1989). In

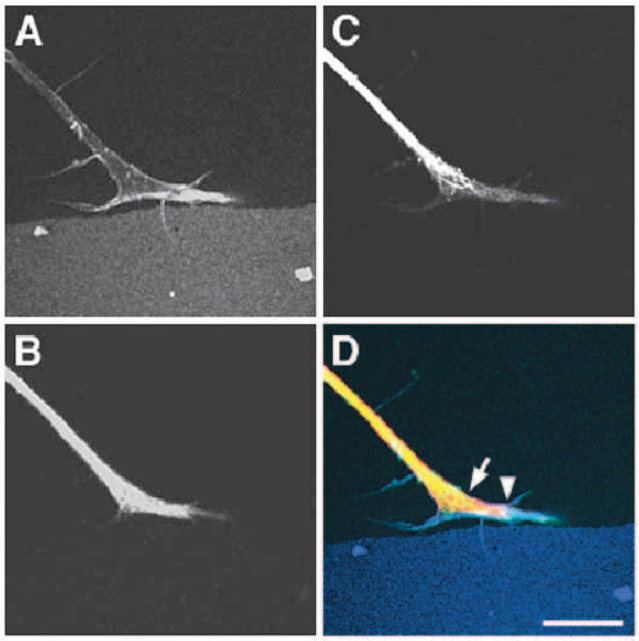

Fig. 3. Arrangement of AFs and MTs in a turning growth cone. (A) phalloidin-labeled AFs; (B) anti-tyrosinated α-tubulin; (C) anti-detyrosinated α-tubulin. The image of detyrosinated α-tubulin staining (C) shows some dim non-specific fluorescence in the distal region of the growth cone, due to the secondary antibody. This can be distinguished from the more proximal specific staining of detyrosinated α-tubulin, which shows intensely labeled MT loops. (D) Merged image of stable MTs (green), dynamic MTs (red) and AFs (blue). The CSPG stripe (also fluorescently labeled, A and D) was enhanced to make it more visible in the images. Tightly bundled dynamic MTs (red) extend into actin-dense regions (blue) at the growth cone tip (D, arrowhead). Stable MTs (green) do not extend as far forward as dynamic MTs (D, arrow). Bar, 10 μm.

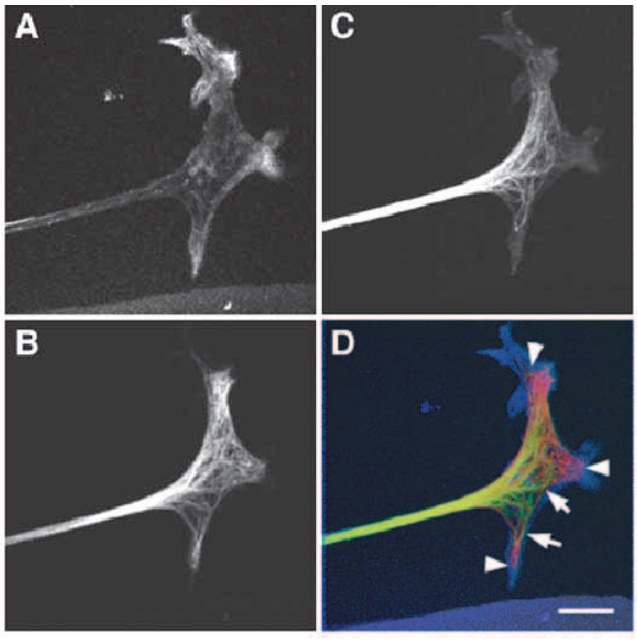

Fig. 4. Distribution of AFs and MTs in a growth cone that turned at a FN/CSPG border and was migrating on FN. (A) phalloidin-labeled AFs; (B) anti-tyrosinated α-tubulin; (C) anti-detyrosinated α-tubulin. (D) Merged image of stable MTs (green), dynamic MTs (red) and AFs (blue). Stable MTs are confined to the central region, where they form loops (D, arrows), while dynamic MTs overlap with AFs at the bases of filopodia (D, arrowheads). Bar, 10 μm.

order to confirm that the altered growth cone behavior and cytoskeletal organization produced by CB treatment was due to disruption of AF bundles, we did analogous experiments using a low concentration (25 ng/ml) of latrunculin B (data not shown). Results show that latrunculin B and CB have the same effects on growth cone morphology, behavior, and configuration of actin and dynamic MTs.

DISCUSSION

Organization of AFs and MTs in turning growth cones

In the experiments reported here we investigated the cytoskeletal events that accompany chick DRG growth cone turning to avoid substratum-bound CSPG. Time-lapse recordings show that when growth cones contacted CSPG, their filopodia sampled it repeatedly by extending and retracting, and in a process that sometimes occurred over several hours, the vast majority of growth cones turned. Confocal images showed that AFs were present in filopodia that crossed the border, while in over 100 growth cones examined dynamic MTs extended to the border but did not cross it (arrowheads in Fig. 2B).

To quantitatively assess MT organization in turning growth cones, we measured several parameters and compared them to similar measurements in growth cones migrating on FN. This analysis revealed two significant changes in MT organization that accompany turning: bundling of MTs and closer association of dynamic MTs with the leading edge, which is rich in AFs.

How are these changes in MT organization regulated at the

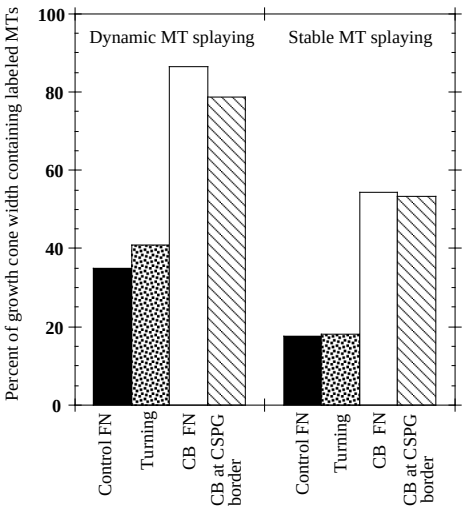

Fig. 5. Degree of growth cone MT splaying. For control growth cones migrating on FN (filled bars), turning at CSPG borders (stippled bars), and CB-treated growth cones migrating on FN (open bars) and either interacting with a CSPG border or sidestepping (hatched bars), the *y*-axis shows percentage values representing the degree of MT splaying. These values were calculated from the data in Table 1. For both dynamic and stable MTs, the degree of MT splaying was estimated by dividing the greatest width of the MT staining by the greatest width of the growth cone. The MTs in CB-treated growth cones are more splayed than in untreated growth cones.

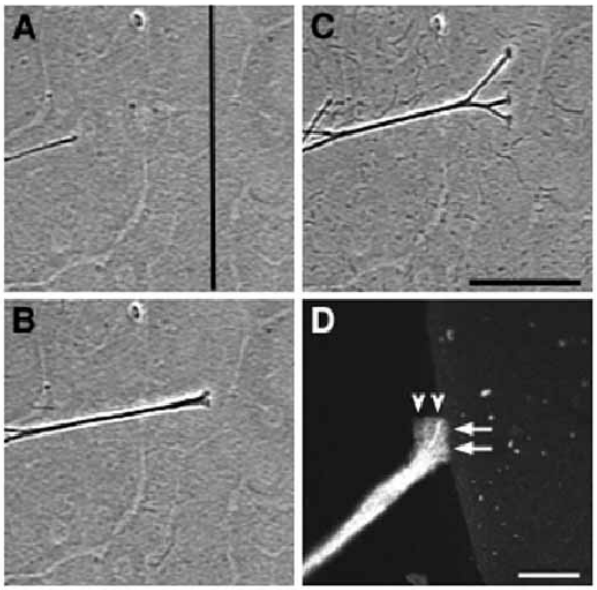

Fig. 6. Growth cone sidestepping in the presence of 0.1 μg/ml cytochalasin B. Phase contrast images of a fascicle containing three growth cones approaching a FN/CSPG border (black line in A), stopped at the border (B), and after two of the growth cones sidestepped along the border by 38 μm (top growth cone) and 17.6 μm (bottom growth cone) (C). The middle growth cone remained at the position shown in B. (D) Confocal image of anti-tyrosinated α-tubulin staining of the top growth cone in C. Dynamic MTs do not extend onto the fluorescently labeled CSPG stripe (D, arrows), and splay with some ends facing the direction of movement (D, arrowheads). Bars: (C) 100 μm; (D) 10 μm.

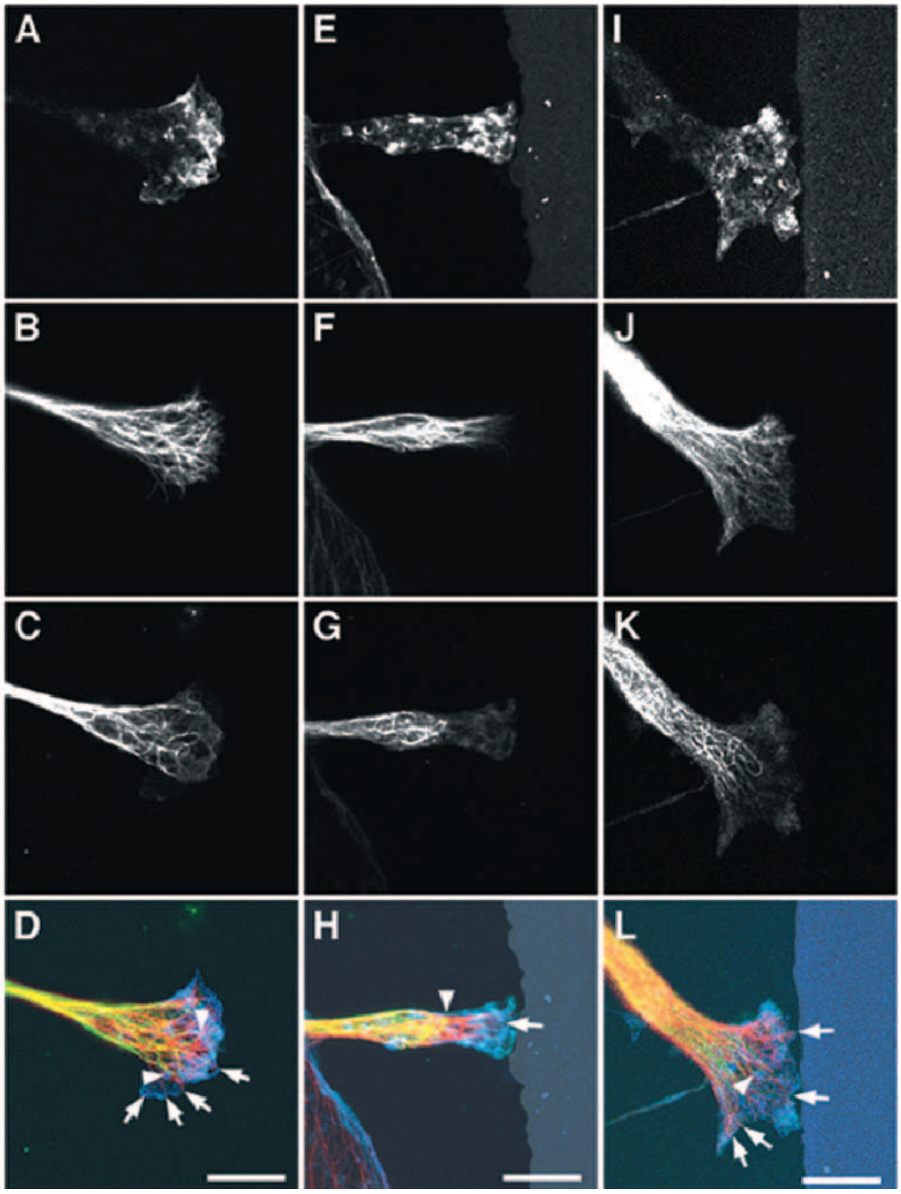

Fig. 7. Triple immunofluorescence of AFs and MTs in growth cones treated with 0.1 μg/ml cytochalasin B and migrating on FN (A-D), at a FN/CSPG border (E-H) and sidestepping to avoid the border (I-L). (A,E,I) Phalloidin-labeled AFs; (B,F,J) tyrosinated α-tubulin (C,G,K) detyrosinated α-tubulin. (D,H,L) Merged images of stable MTs (green), dynamic MTs (red) and AFs (blue). The CSPG stripe (E,I,H,L) was enhanced to make it more visible in the images. When the growth cone AF network is reduced by cytochalasin B, dynamic MTs are closer to the leading edge, which contains punctate actin staining (D,H,L, arrows). Looped stable MTs overlap with dynamic MTs, but are generally excluded from the actin-dense regions (D,H,L, arrowheads). In growth cones at a CSPG border, dynamic MTs stop at the border (H, L). Growth cones avoiding CSPG by sidestepping (L) contain MTs that are not as tightly bundled as those in untreated growth cones that are turning (see Fig. 3D). Bar, 10 μm.

front of turning growth cones? Two possibilities are: (1) regulation of MT advance via polymerization/depolymerization and translocation; and (2) regulation of MT bundling, degree of splaying and orientation. Both polymerization and translocation contribute to MT advance (Edson et al., 1993; Joshi and Baas, 1993; Reinsch et al., 1991; Sabry et al., 1991; Tanaka and Sabry, 1995; Tanaka and Kirschner, 1991). However, the relative contribution of each of these mechanisms differs among neuronal types (Okabe and Hirokawa, 1992). The MTs are very dynamic in DRG growth cones, while more proximally along DRG neurites, the MT cytoskeleton is largely stationary (Edson et al., 1993; Okabe and Hirokawa, 1992).

Our immunocytochemical results are consistent with the interpretation that MTs advance by both polymerization and translocation, since the MT ends that project the farthest forward are all dynamic (labeled solely with anti-tyrosinated α-tubulin) and may advance by polymerization, but the looped stable MTs (labeled preferentially with anti-detyrosinated α-tubulin) probably advance by translocation (Tanaka and Kirschner, 1991). It has been shown recently that low concentrations of taxol inhibit growth cone turning at a LN/tenascin border (Williamson et al., 1995) and at a FN/CSPG border (J. F. Challacombe et al., unpublished), perhaps by reducing the dynamic growth of MT ends into the P-domain (Jordan et al., 1993). These results support the view that dynamic extension of MTs towards the leading edge promotes growth cone turning. Another possible contribution to our finding that dynamic MTs are closer to the leading edge during turning is that the P-domain shrinks. This would also result in a greater association of dynamic MTs with AFs at the leading edge.

The bundling, splaying, and orientation of growth cone MTs may be controlled by microtubule-associated proteins (MAPs) that mediate MT-MT and MT-AF interactions, and by structural interference or forces generated by the AF matrix of the P-domain. MT bundling and stabilization against depolymerization can be mediated by MAP 1b and tau, which are reported to be present in growth cones (Diaz-Nido et al., 1992; DiTella et al., 1994; Mansfield et al., 1991), and may also bind to actin (Correas et al., 1990; Fujii et al., 1993; Selden and Pollard, 1983). A MAP-mediated linkage between dynamic MT ends and AFs would allow the tensions generated by the AF matrix in the P-domain to pull on MT ends and regulate MT orientation. Conversely, structural interference or forces associated with the AF network may inhibit MT splaying and advance. Tensions within the cortical AF matrix and in the lamellar AF network tend to confine MTs to the central domain (Lamoureux et al., 1990; Letourneau et al., 1987). In addition, retrograde flow of AFs from the leading edge may restrict MT spreading into the P-domain (Lin and Forscher, 1995).

Role of AFs in growth cone turning

To test our hypothesis that AFs in the growth cone P-domain regulate MT advance, bundling, and orientation during growth cone turning, we used a low concentration of the AF-disrupting drug CB that reduced protrusive activity of the leading margin, but allowed growth cone migration to continue (Letourneau et al., 1987). CB-treated growth cones migrating on homogeneous FN contained dynamic and stable MTs that were more splayed and were closer to the leading edge than in control growth cones. Assuming that CB reduces the density and forces produced in the AF matrix, these results support the idea that the AF matrix and its associated tensile forces and retrograde flow confine MT spreading and advance. When CB-treated growth cones encounter a border with CSPG, they do not turn; instead, they sidestep laterally along the border, remain symmetric, and splayed MTs are even closer to the front margin. Most importantly, MTs are not bundled or oriented to one side, as in turning growth cones.

These effects of CB indicate that the splaying of MTs throughout the P-domain and their close proximity to the leading edge are not sufficient for growth cone turning. Rather, we propose that MTs must be oriented to one side of the growth cone by interactions with AF bundles. This hypothesis is consistent with our previous EM observations (Letourneau, 1979; Letourneau and Ressler, 1983; Letourneau et al., 1987), as well as the work of others (Bentley and O'Connor, 1994; Lin and Forscher, 1993; Lin and Forscher, 1995; O'Connor and Bentley, 1993). AFs may also play a role in anchoring the growth cone to FN, because reducing AFs results in sidestepping, a behavior that has been attributed to decreased adhesion to the substratum (Tanaka and Kirschner, 1995).

The results of these investigations are new, because they provide evidence that AF bundles are necessary for the MT reorganization that is crucial for growth cone turning to avoid an inhibitory cue. Previous studies of growth cone interactions with in vivo guideposts (Bentley and O'Connor, 1994; O'Connor and Bentley, 1993) and in vitro targets (Lin and Forscher, 1993) showed that MTs advance and orient toward AF bundles that are linked to a contact with a positive cue. However, experimental disruption of AF bundles was examined only in the study addressing target contact. With regard to growth cone turning, it was not asked whether AF bundles were required for the orientation of MTs toward the positive cue. Our results show that CB-treated growth cones without AF bundles are unable to turn to avoid an inhibitory cue. Instead, they sidestep laterally and maintain a symmetric, widespread distribution of MTs.

Growth cone turning is an important behavior in axonal pathfinding that may involve several distinct mechanisms, i.e. localized growth cone collapse (Fan et al., 1993), localized growth cone advance (Bentley and O'Connor, 1994), branching or backbranching (Goldberg and Burmeister, 1986). Which turning mechanism operates will depend on the guidance cues that exist in each situation. Our results indicate that an essential activity in growth cone turning to avoid CSPG is the bundling and alignment of MTs by interactions with AF bundles.

We thank Drs M. L. Condic and P. J. Sammak for suggestions on the manuscript, Drs A. I. Caplan and D. A. Carrino for continued support and supply of chick limb bud CSPG, and Drs J. C. Bulinski and G. G. Gundersen for antiserum against detyrosinated α-tubulin. This work was supported by NIH grants HD19950 (P.C.L.), EY10545 (D.M.S.), and F32-NS09971 (J.F.C.), NSF training grant DIR-9113444, and the Minnesota Medical Foundation.

REFERENCES

Arregui, C., Busciglio, A., Caceres, A. and Barra, H. S. (1991). Tyrosinated and detyrosinated microtubules in axonal processes of cerebellar macroneurons grown in culture. *J. Neurosci. Res.* **28**, 171-181.

Baas, P. W. and Black, M. M. (1990). Individual microtubules in the axon consist of domains that differ in both composition and stability. *J. Cell Biol.* **111**, 495-509.

Baas, P. W., Ahmad, F. J., Pienkowski, T. P., Brown, A. and Black, M. M.

(1993). Sites of microtubule stabilization for the axon. *J. Neurosci.* **13**, 2177-2185.

Bentley, D. and Toroian-Raymond, A. (1986). Disoriented pathfinding by pioneer neuron growth cones deprived of filopodia by cytochalasin treatment. *Nature* **323**, 712-715.

Bentley, D. and O'Connor, T. P. (1994). Cytoskeletal events in growth cone steering. *Curr. Opin. Neurobiol.* **4**, 43-48.

Brelje, T. C., Wessendorf, M. W. and Sorenson, R. L. (1993). Multicolor laser scanning confocal immunofluorescence microscopy: practical applications and limitations. *Meth. Cell Biol.* **38**, 97-181.

Bridgman, P. C. (1992). Functional anatomy of the growth cone in relation to its role in locomotion and neurite assembly. In *The Nerve Growth Cone* (ed. P. C. Letourneau, E. R. Macagno and S. B. Kater), pp. 39-54. Raven Press, New York.

Brittis, P. A., Canning, D. R. and Silver, J. (1992). Chondroitin sulfate as a regulator of neuronal patterning in the retina. *Science* **255**, 733-736.

Brown, A., Li, Y., Slaughter, T. and Black, M. M. (1993). Composite microtubules of the axon: quantitative analysis of tyrosinated and acetylated tubulin along individual axons. *J. Cell Sci.* **104**, 339-352.

Carrino, D. A. and Caplan, A. I. (1985). Isolation and characterization of proteoglycans synthesized in ovo by embryonic chick cartilage and new bone. *J. Biol. Chem.* **260**, 122-127.

Challacombe, J. F., Snow, D. M. and Letourneau, P. C. (1995). Growth cone filopodia detect navigational cues while microtubules execute directional changes. *Soc. Neurosci. Abs* **21**, 13.

Chien, C.-B., Rosenthal, D. E., Harris, W. A. and Holt, C. E. (1993). Navigational errors made by growth cones without filopodia in the embryonic Xenopus brain. *Neuron* **11**, 237-251.

Cooper, J. A. (1987). Effects of cytochalasin and phalloidin on actin. *J. Cell Biol.* **105**, 1473-1478.

Correas, I., Padilla, R. and Avila, J. (1990). The tubulin-binding sequence of brain microtubule-associated proteins, tau and MAP-2, is also involved in actin binding. *Biochem. J.* **269**, 61-64.

Diaz-Nido, J., Armas-Portela, R., Martinez, A., Rocha, M. and Avila, J. (1992). Role of microtubules in neurite outgrowth. In *The Nerve Growth Cone* (ed. P. C. Letourneau, E. R. Macagno and S. B. Kater), pp. 65-77. Raven Press, Ltd, New York.

DiTella, M., Feiguin, F., Morfini, G. and Caceres, A. (1994). Microfilament-associated growth cone component depends upon tau for its intracellular localization. *Cell Motil. Cytoskel.* **29**, 117-130.

Edson, K. J., Lim, S.-S., Borisy, G. G. and Letourneau, P. C. (1993). FRAP analysis of the stability of the microtubule population along the neurites of chick sensory neurons. *Cell Motil. Cytoskel.* **25**, 59-72.

Fan, J., Mansfield, G., Redmond, T., Gordon-Weeks, P. R. and Raper, J. A. (1993). The organization of F-actin and microtubules in growth cones exposed to a brain-derived collapsing factor. *J. Cell Biol.* **121**, 867-878.

Forscher, P. and Smith, S. J. (1988). Actions of cytochalasins on the organization of actin filaments and microtubules in a neuronal growth cone. *J. Cell Biol.* **107**, 1505-1516.

Fujii, T., Watanabe, M., Ogoma, Y., Kondo, Y. and Arai, T. (1993). Microtubule-associated proteins, MAP 1A and MAP 1B, interact with F-actin in vitro. *J. Biochem.* **114**, 827-829.

Goldberg, D. J. and Burmeister, D. W. (1986). Stages in axon formation: observations of growth of Aplysia axons in culture using video-enhanced contrast-differential interference contrast microscopy. *J. Cell Biol.* **103**, 1921-1931.

Goodman, C. S., Grenningloh, G. and Bieber, A. J. (1992). Molecular genetics of neural cell adhesion molecules in *Drosophila*. In *The Nerve Growth Cone* (ed. P. C. Letourneau, E. R. Macagno and S. B. Kater), pp. 283-304. Raven Press, New York.

Gordon-Weeks, P. R. (1991). Evidence for microtubule capture by filopodial actin filaments in growth cones. *NeuroReport* **2**, 573-576.

Gundersen, G. G., Kalnoski, M. H. and Bulinski, J. C. (1984). Distinct populations of microtubules: tyrosinated and nontyrosinated alpha tubulin are distributed differently in vivo. *Cell* **38**, 779-789.

Jordan, M. A., Toso, R. J., Thrower, D. and Wilson, L. (1993). Mechanism of mitotic block and inhibition of cell proliferation by taxol at low concentrations. *Proc. Nat. Acad. Sci. USA* **90**, 9552-9556.

Joshi, H. C. and Baas, P. W. (1993). A new perspective on microtubules and axon growth. *J. Cell Biol.* **121**, 1191-1196.

Kennedy, T. E. and Tessier-Lavigne, M. (1995). Guidance and induction of branch formation in developing axons by target-derived diffusible factors. *Curr. Opin. Neurobiol.* **5**, 83-90.

Kilmartin, J. V., Wright, B. and Milstein, D. (1982). Rat monoclonal antitubulin antibodies derived using a new non-secretory rat cell line. *J. Cell Biol.* **9**, 3576-3582.

Lagenaur, C. and Lemmon, V. (1987). An L1-like molecule, the 8D9 antigen is a potent substrate for neurite extension. *Proc. Nat. Acad. Sci. USA* **84**, 7753-7757.

Lamoureux, P., Steel, V. L., Regal, C., Adgate, L., Buxbaum, R. E. and Heidemann, S. R. (1990). Extracellular matrix allows neurite elongation in the absence of microtubules. *J. Cell Biol.* **110**, 71-79.

Letourneau, P. C. (1979). Cell-substratum adhesion of neurite growth cones, and its role in neurite elongation. *Exp. Cell Res.* **124**, 127-138.

Letourneau, P. C. and Ressler, A. H. (1983). Differences in the organization of actin in the growth cones compared with the neurites of cultured neurons from chick embryos. *J. Cell Biol.* **97**, 963-973.

Letourneau, P. C., Shattuck, T. A. and Ressler, A. H. (1987). 'Pull' and 'push' in neurite elongation: observations on the effects of different concentrations of cytochalasins and taxol. *Cell Motil. Cytoskel.* **8**, 193-209.

Letourneau, P. C. and Shattuck, T. A. (1989). Distribution and possible interactions of actin-associated proteins and cell adhesion molecules of nerve growth cones. *Development* **105**, 505-519.

Letourneau, P. C., Shattuck, T. A., Roche, F. K., Takeichi, M. and Lemmon, V. (1990). Nerve growth cone migration onto Schwann cells involves the calcium-dependent adhesion molecule, N-cadherin. *Dev. Biol.* **138**, 430-442.

Letourneau, P. C. (1992). Integrins and N-cadherin are adhesive molecules involved in growth cone migration. In *The Nerve Growth Cone* (ed. P. C. Letourneau, E. R. Macagno and S. B. Kater), pp. 181-194. Raven Press, New York.

Letourneau, P. C., Condic, M. L. and Snow, D. M. (1994). Interactions of developing neurons with the extracellular matrix. *J. Neurosci.* **14**, 915-928.

Lewis, A. K. and Bridgman, P. C. (1992). Nerve growth cone lamellipodia contain two populations of actin filaments that differ in organization and polarity. *J. Cell Biol.* **119**, 1219-1243.

Lin, C.-H. and Forscher, P. (1993). Cytoskeletal remodeling during growth cone-target interactions. *J. Cell Biol.* **121**, 1369-1383.

Lin, C.-H. and Forscher, P. (1995). Growth cone advance is inversely proportional to retrograde F-actin flow. *Neuron* **14**, 763-771.

Lin, C.-H., Thompson, C. A. and Forscher, P. (1994). Cytoskeletal reorganization underlying growth cone motility. *Curr. Opin. Neurobiol.* **4**, 640-647.

Lumsden, A. (1992). Chemotaxis in the developing nervous systems of vertebrates. In *The Nerve Growth Cone* (ed. P. C. Letourneau, E. R. Macagno and S. B. Kater), pp. 167-180. Raven Press, New York.

MacLean-Fletcher, S. and Pollard, T. D. (1980). Mechanism of action of cytochalasin B on actin. *Cell* **20**, 329-341.

Mansfield, S. G., Diaz-Nido, J., Gordon-Weeks, P. R. and Avila, J. (1991). The distribution and phosphorylation of the microtubule-associated protein MAP 1B in growth cones. *J. Neurocytol.* **20**, 1007-1022.

Marsh, L. and Letourneau, P. C. (1984). Growth of neurites without filopodial or lamellipodial activity in the presence of cytochalasin B. *J. Cell Biol.* **99**, 2041-2047.

McKeon, R. J., Schreiber, R. C., Rudge, J. S. and Silver, J. (1991). Reduction of neurite outgrowth in a model of glial scarring following CNS injury is correlated with the expression of inhibitory molecules on reactive astrocytes. *J. Neurosci.* **11**, 3398-3411.

Meiners, S., Powell, E. M. and Geller, H. M. (1995). A distinct subset of Tenascin/CS-6-PG-rich astrocytes restricts neuronal growth in vitro. *J. Neurosci.* **15**, 8096-8108.

Mitchison, T. and Kirschner, M. (1988). Cytoskeletal dynamics and nerve growth. *Neuron* **1**, 761-772.

Mosteller, F. and Rourke, R. E. K. (1973). *Sturdy Statistics. Nonparametrics and Order Statistics.* Addison-Wesley Publishing Company.

O'Connor, T. P. and Bentley, D. (1993). Accumulation of actin in subsets of pioneer growth cone filopodia in response to neural and epithelial guidance cues in situ. *J. Cell Biol.* **123**, 935-948.

O'Leary, D. D., Heffner, C. D., Kutka, L., Lopez-Mascaraque, L., Missias, A. and Reinoso, B. S. (1991). A target-derived chemoattractant controls the development of the corticopontine projection by a novel mechanism of axon targeting. *Development Suppl. 2*, 123-130.

Oakley, R. A. and Tosney, K. W. (1991). Peanut agglutinin and chondroitin-6-sulfate are molecular markers for tissues that act as barriers to axon advance in the avian embryo. *Dev. Biol.* **147**, 187-206.

Okabe, S. and Hirokawa, N. (1992). Differential behavior of photoactivated microtubules in growing axons of mouse and frog neurons. *J. Cell Biol.* **117**, 105-120.

Pindzola, R. R., Doller, C. and Silver, J. (1993). Putative inhibitory extracellular matrix molecules at the dorsal root entry zone of the spinal cord during development and after root and sciatic nerve lesions. *Dev. Biol.* **156**, 34-48.

Reichardt, L. F. and Tomaselli, K. J. (1991). Extracellular matrix molecules and their receptors: functions in neural development. *Annu. Rev. Neurosci.* **14**, 531-570.

Reinsch, S. S., Mitchison, T. J. and Kirschner, M. W. (1991). Microtubule polymer assembly and transport during axonal elongation. *J. Cell Biol.* **115**, 365-380.

Sabry, J. H., O'Connor, T. P., Evans, L., Toroian-Raymond, A., Kirschner, M. and Bentley, D. (1991). Microtubule behavior during guidance of pioneer neuron growth cones in situ. *J. Cell Biol.* **115**, 381-395.

Sanes, J. R. (1989). Extracellular matrix molecules that influence neural development. *Annu. Rev. Neurosci.* **12**, 491-516.

Schliwa, M. and van Blerkom, J. (1981). Structural interaction of cytoskeletal components. *J. Cell Biol.* **90**, 222-235.

Selden, S. C. and Pollard, T. D. (1983). Phosphorylation of microtubule-associated proteins regulates their interaction with actin filaments. *J. Biol. Chem.* **258**, 7064-7071.

Smith, C. L. (1994). Cytoskeletal movements and substrate interactions during initiation of neurite outgrowth by sympathetic neurons *in vitro*. *J. Neurosci.* **14**, 384-398.

Snow, D. M., Lemmon, V., Carrino, D. A., Caplan, A. I. and Silver, J. (1990). Sulfated proteoglycans in astroglial barriers inhibit neurite outgrowth *in vitro*. *Exp. Neurol.* **109**, 111-130.

Snow, D. M., Watanabe, M., Letourneau, P. C. and Silver, J. (1991). A chondroitin sulfate proteoglycan may influence the direction of retinal ganglion cell outgrowth. *Development* **113**, 1473-1485.

Snow, D. M. and Letourneau, P. C. (1992). Neurite outgrowth on a step gradient of chondroitin sulfate proteoglycan (CS-PG). *J. Neurobiol.* **23**, 322-336.

Snow, D. M., Atkinson, P. B., Hassinger, T. D., Letourneau, P. C. and Kater, S. B. (1994). Chondroitin sulfate proteoglycan elevates cytoplasmic calcium in DRG neurons. *Dev. Biol.* **166**, 87-100.

Spector, I., Shochet, N. R., Blasberger, D. and Kashman, Y. (1989). Latrunculins-novel marine macrolides that disrupt microfilament organization and affect cell growth: I. Comparison with cytochalasin D. *Cell Motil. Cytoskel.* **13**, 127-144.

Sretavan, D. W. and Reichardt, L. F. (1993). Time-lapse video analysis of retinal ganglion cell axon pathfinding at the mammalian optic chiasm: growth cone guidance using intrinsic chiasm cues. *Neuron* **10**, 761-777.

Tanaka, E. M. and Kirschner, M. W. (1991). Microtubule behavior in the growth cones of living neurons during axon elongation. *J. Cell Biol.* **115**, 345-363.

Tanaka, E. and Kirschner, M. W. (1995). The role of microtubules in growth cone turning at substrate boundaries. *J. Cell Biol.* **128**, 127-137.

Tanaka, E. and Sabry, J. (1995). Making the connection: cytoskeletal rearrangements during growth cone guidance. *Cell* **83**, 171-176.

Webster, D. R., Gundersen, G. G., Bulinski, J. C. and Borisy, G. G. (1987). Differential turnover of tyrosinated and detyrosinated microtubules. *Proc. Nat. Acad. Sci. USA* **84**, 9040-9044.

Williamson, T., Gordon-Weeks, P. R., Schachner, M. and Taylor, J. (1995). Microtubule reorganisation is obligatory for growth cone turning. *Soc. Neurosci. Abs* **21**, 1775.

(Received 5 February 1996 – Accepted 2 May 1996)